Validation of the inverted adsorption structure for 2H-tetraphenyl porphyrin on Cu(111)

P.T.P. Ryan[1,2], P. L. Lalaguna[1,3], F. Haag[4], M. M. Braim[5], P. Ding[5,6], D. J. Payne[2] J. V. Barth[4], T.-L. Lee[1], D. P. Woodruff[5], F. Allegretti[4] and D. A. Duncan[1]*

1. Diamond Light Source, Harwell Science and Innovation Campus, Didcot, OX11 0QX, United Kingdom

2. Department of Materials, Imperial College London, SW7 2AZ, UK.

3. School of Chemistry, University of Glasgow, G12 8QQ, UK

4. Physics Department E20, Technical University of Munich, James Franck Straße 1, D-85748 Garching, Germany

5. Department of Physics, University of Warwick, Coventry, CV4 7AL, UK

6. State Key Laboratory of Urban Water Resource and Environment, School of Chemistry and Chemical Engineering, Harbin Institute of Technology, Harbin 150001, China

Supplementary Information

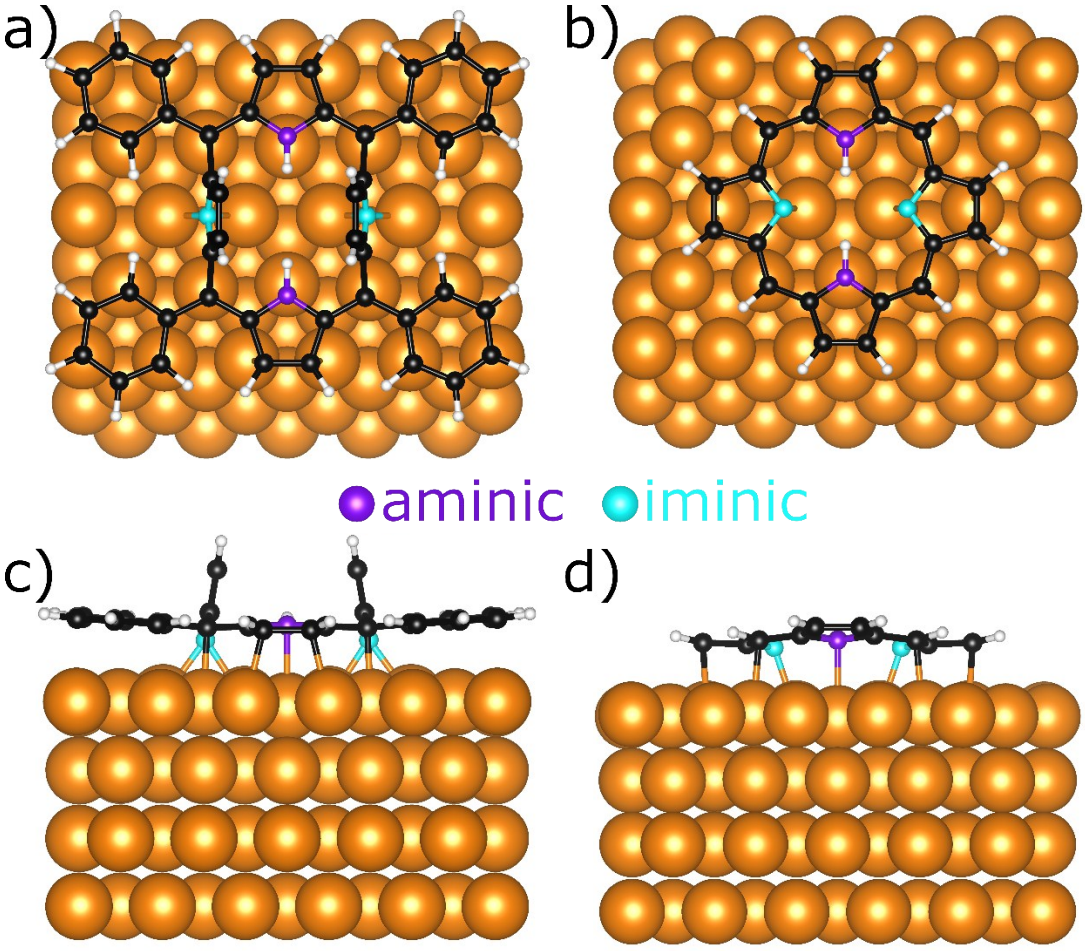

Figure S1. Schematic of the (a,c) inverted model of 2H-TPP adsorbed on Cu(111), adapted from Ref. [1] with permission from The Royal Society of Chemistry, and (b,d) the determined adsorption structure of 2H-P on Cu(111), adapted from Ref. [2] with permission from AIP Publishing. The structural models are shown in (a,b) a plan and (c,d) side view. Aminic N atoms, iminic N atoms, C atoms, H atoms and Cu atoms are shown as purple, cyan, black, white and copper spheres, respectively.

Further experimental details

The I09 beam line consists of two separate undulators that can simultaneously deliver soft (0.11 to 2.00 keV) and hard (2.15 to 15.00 keV) X-ray radiation onto the same spot on the sample in the ultra-high vacuum end station. The end station utilises a Scienta EW4000 HAXPES analyser for acquiring X-ray photoelectron spectroscopy (XPS)

data at 'soft' photon energies with higher spectral resolution (SXPS) and at the 'harder' energies required. to record the NIXSW data. This analyser, with an acceptance angle of approximately ±30°, was mounted perpendicular to the incident hard X-rays in the horizontal plane of the photon linear polarisation.

The (111) planes that are parallel to the surface at a normal incidence Bragg energy of $h\nu$ = 2.63 keV; reflection from the $(\bar{1}11)$ planes that are tilted by an angle of ~70° with respect to the surface, also at a normal incidence Bragg energy of $h\nu$ = 2.63 keV; and reflection from the (200) planes that are tilted by an angle of ~55° with respect to the surface with a corresponding normal incidence Bragg energy of $h\nu$ = 3.43 keV. Each individual NIXSW measurement was performed rapidly (~20 minutes) and multiple repeated measurements were acquired from different spots on the sample. On each individual spot the reflectivity curve was measured to ascertain the crystalline quality of that spot and allow exact energy alignment of the individual NIXSW measurements that were summed to improve the signal-to-noise ratio. The total number of NIXSW spectra acquired for the (111) reflection was 31 N 1s and 7 C 1s, for the $(\bar{1}11)$ reflection 28 N 1s and 10 C 1s, and for the (200) reflection 22 N 1s and 7 C 1s.

The Cu(111) crystal (Surface Preparation Laboratory) was cleaned by repeated cycles of sputtering and annealing (~750 K) cycles. Cleanliness was assessed by SXPS. Throughout the study a degree of persistent carbon contamination was observed, although this was minimised by alternately annealing the Cu crystal *in vacuo* and in an oxygen partial pressure during cleaning cycles. 2H-TPP was deposited onto the surface, that was held at room temperature, using a commercial organic molecular beam evaporator (MBE Komponenten, OEZ 40-2x1). To monitor the coverage, we compared the N 1s SXPS intensity of our overlayer preparations to that of a complete monolayer of 2H-TPP on Ag(111). Using this calibration we estimated the coverages on Cu(111) to vary between 0.4 and 0.6 ML for different preparations (where 1 ML is defined as a saturated monolayer of 2H-TPP on Ag(111)), resulting in an approximate molecular flux of 1-2 mML/s.

NIXSW measurements of the absorption rate of the C and N atoms were acquired at the (111), $(\bar{1}11)$ and (200) substrate reflections (shown, with respect to the (111) surface plane, in Figure 1b), monitoring the N 1s and C 1s photoemission intensities. Non-dipolar effects in the angular dependence of the high-energy photoemission were corrected as described in ref. [3] using a value of the backward-forward asymmetry parameter, Q,[4] derived from the theoretical calculations of ref [5]. It was assumed that these non-dipolar effects in the measurements using a wide angular range of emission detection could be modelled by a mean value of the emission angle, θ, defined as the angle between the photon polarisation and the photoelectron detection direction. In all cases only emission at angles lying between the photon polarisation and the vector normal to the probed scatterer planes were used (i.e. values θ > 0 were included, θ < 0 were excluded). For the $(\bar{1}11)$ and (200) reflections the Q parameter was calculated using a value of θ of 15°. For the (111) reflection the experimental geometry meant that the accepted angular range of the analyser included 90° grazing emission that is strongly attenuated so a slightly larger value of θ of 18° was used.

Role of sample preparation

In the publication of Albrecht et al.[6] it was suggested that differences in sample preparation may account for the different conclusions regarding the conformation of the molecule between their work and that of Diller et al.. Summarising these conditions briefly, substrate temperatures for deposition were 220 K (Diller et al.[7]), 10 K (Albrecht et al.[6]), unspecified (Bürker et al.[8]) and room temperature (Lepper et al.[1] and Moreno-López et al.[9]); the estimated coverage reported by Diller et al. was 1 ML (defined by them as a saturated single layer), but Bürker et al., Albrecht et al., Lepper et al. and Moreno-López et al do not state what coverage was used in their studies, although single-molecule STM images suggest their likely coverages were << 1 ML. As the STM work of Albrecht et al., Lepper et al. and Moreno-López et al., as well as the NIXSW work presented here, identify the presence of the inverted model, it seems clear that substrate temperature cannot play a significant role in its formation. However, the different coverages could, indeed, be the reason for this discrepancy. In particular, Diller et al. present the only study that was performed at near 1 ML coverage. In the DFT calculations of Lepper et al.[1] the predicted charge transfer into the molecule, from the substrate, was -1.91 e for the inverted model, whereas for the saddle shape model, a much smaller charge transfer (-0.08 e into the molecule) was predicted. In a densely packed island such a large charge transfer into the molecule from the surface may no longer be energetically favourable, so very high coverages may force the molecule into the saddle shape conformation. Notably, at higher coverages, there is a distinct difference in the packing of the molecular layer, the so-called checkerboard structure[10]. In the work of Röckert et al.[11] they present N 1s XP spectra of both a sub-monolayer coverage (comparable to the work presented here) and of a coverage that would correspond to a checkerboard structure, which show slight differences in binding energy shift between the two N species (iminic and aminic). By directly comparing the differences in photoelectron binding energy

between the spectra of Fig. 2 of Röckert et al. and Fig. 2b of Diller et al., we see that the latter agrees better with that of a low coverage of the 2H-TPP than with that of the checkerboard structure. This raises the question of whether the determinations of coverage in these two studies are comparable. Diller et al. specified their coverage by comparing the measured XPS intensities relative to those obtained from a multilayer of 2H-TPP on Cu(111) annealed to 550 K. In this work, we specify our coverage by comparing the XPS intensities relative to those measured from a multilayer of 2H-TPP on Ag(111). Bürker et al. calculate their coverage using the intensity ratio of the C 1s and Cu $3p_{3/2}$ and the approximate size of the unit cell occupied by a TPP molecule.

It is not clear that annealing a multilayer of 2H-TPP on Cu(111) would result in the densely packed checkerboard structure; in fact close inspection of the XP spectra in Fig. 2 of Röckert et al.[11] suggests that annealing the checkerboard structure to ~500 K results in a notable decrease (by ~20%) in intensity of both the N 1s and C 1s intensities. In the work of Röckert et al. the XP spectra of the checkerboard structure were acquired at a coverage of 0.50 molecules nm^{-2}, while the STM image from a coverage of 0.43 molecules nm^{-2} (14% lower) appears to show coexistence of the checkerboard structure and the more disordered lower coverage phase. Finally, according to the paper of Röckert et al., only the lower coverage phase should be present below a coverage of 0.37 molecules nm^{-2} (26% lower). If the higher coverage checkerboard structure has a lower adsorption energy per molecule than the disordered phase, as one might expect, it may not be surprising if the coverage of the 2H-TPP decreases upon annealing at a temperature sufficient to remove a multilayer. Therefore, it is conceivable that the 1 ML quoted by Diller et al. is instead the highest possible coverage of the disordered 2H-TPP phase, the same phase that was studied in this work, and was studied by Bürker et al., Albrecht et al., Lepper et al. and Moreno-López et al..

If differences in coverage cannot explain the discrepancy between the conclusions derived from the NEXAFS measurements and from the STM, DFT and NIXSW studies, the other possible problem lies in the analysis of the NEXAFS data. In order to guide their analyses, Diller et al. utilised DFT calculations of an isolated 2H-TPP molecule to assign the features they observed in both their C K-edge and N K-edge NEXAFS. Though they only directly applied the DFT calculations to analysing the multilayer spectra, the insight they gained from doing so was also applied to the monolayer case. Considering the strong interaction between the substrate and the molecule, the potential charge transfer of -1.91 e into the molecule from the substrate, and the significant distortion of the macrocycle in the inverted model, it seems likely that molecular orbitals and associated energies of a 2H-TPP monolayer will differ significantly from those of either an isolated 2H-TPP molecule or a multilayer of 2H-TPP. Indeed, this is reflected in the spectra of Figures 4a and 4b of Diller et al., in which the relative intensity near the magic angle of the peaks B, C, D and E (for a multilayer of 2H-TPP) are completely different from the peaks B', C', D' and E' of the monolayer. Furthermore, more recent DFT calculations into 2H-P by Diller et al.[12] suggest that, should a similar interaction between substrate and adsorbate be present for 2H-TPP, separation of the features in the NEXAFS of 2H-TPP on Cu(111) into discrete species may well be impossible without more stringent fitting parameters from DFT calculations that model the whole adsorbate/substrate system.

In summary, it is possible that the discrepancy between the NEXAFS and the STM, DFT and NIXSW studies is due to the higher coverage in the NEXAFS study, yet this is uncertain due to the ambiguity in how different groups have quoted their relative coverages (and the difficulty, in general, of defining such coverages). As such, a coverage-dependent NEXAFS study could help to resolve this question. What could be even more valuable would be more modern DFT calculations of the expected NEXAFS spectra from the inverted model. A combination of the two studies would be particularly useful to understand what, if any, role higher coverages play in the conformation of 2H-TPP on the surface.

N 1s SXPS radiation damage check

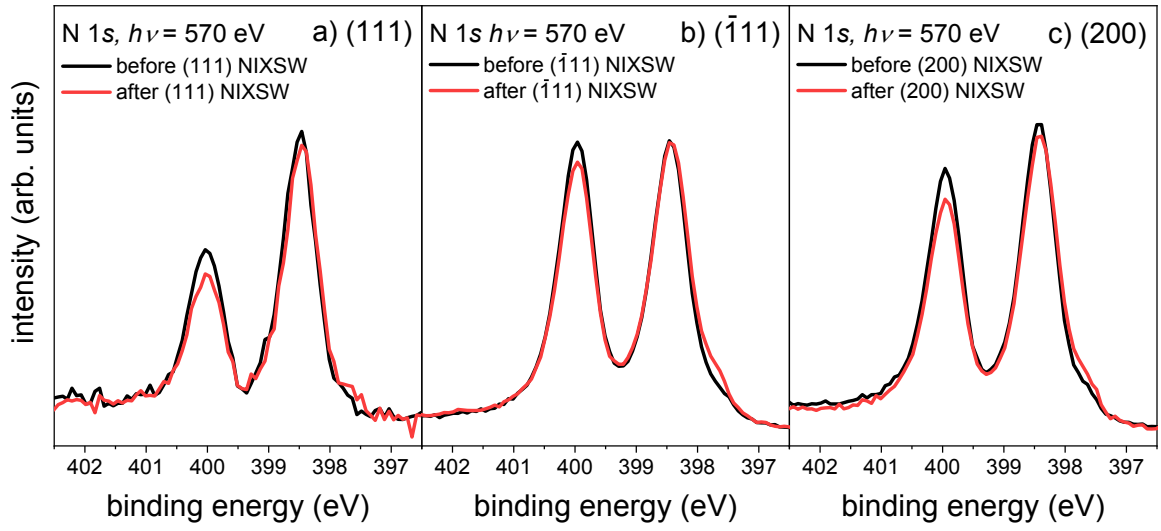

Figure S2. The integrated SXP spectra taken before (black line) and after (red line) every single NIXSW spectrum for the (111), $(\bar{1}11)$ and (200) reflections. At the signal to noise ratio for a single measurement, no beam damage was apparent. The spectra presented here were obtained by integrating 42 (111), 38 $(\bar{1}11)$ and 29 (200) repeated measurements, and show a very small amount of beam damage . Note: changes in relative intensities between the reflections are due to photoelectron diffraction effects in the different collection geometries.

C 1s SXPS and NIXSW

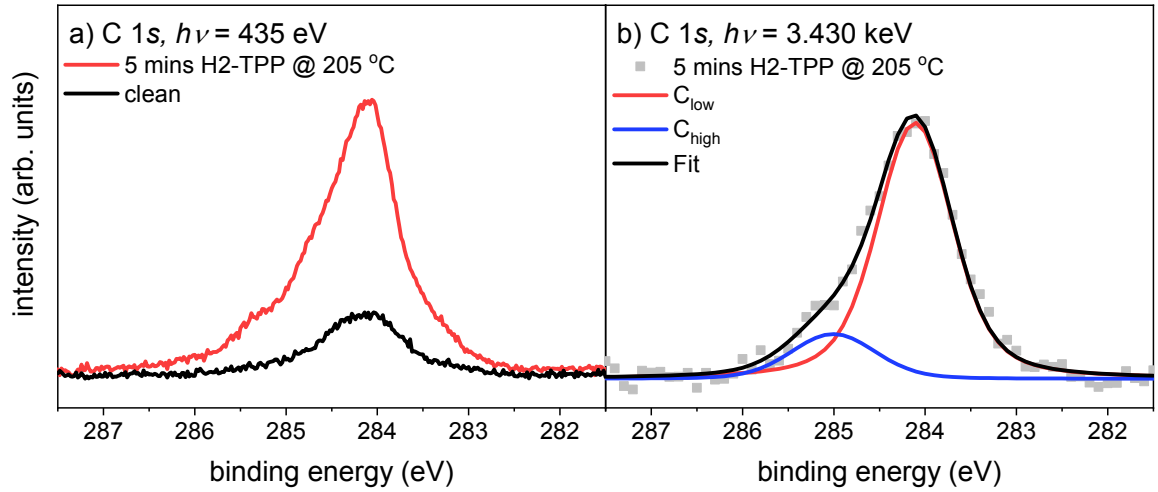

Figure S3. The a) SXPS and b) the fitted HAXPES of the C 1s region. A noticeable carbon contamination remains after cleaning the Cu(111) surface, the associated C 1s XP peak being almost coincident with the lower binding energy C 1s peak from the adsorbed molecule.

Calculation of the 2D single site model maps

The degree of agreement between the measured coherent fractions (f_{hkl}^{exp}) and coherent positions (p_{hkl}^{exp}) and the values of these parameters expected for different absorber atom sites was quantified by the value of the function:

$$\chi = \frac{\sum_{hkl}\left(\frac{\left(f_{hkl}^{exp} - f_{hkl}^{the}\right)^2}{\sigma_{f_{hkl}}^{\ 2}} + \frac{\left(p_{hkl}^{exp} - p_{hkl}^{the}\right)^2}{\sigma_{p_{hkl}}^{\ 2}}\right)}{N \times \sigma_{sum}}, \quad (1)$$

where *N* is the number of measured coherent positions and coherent fractions associated with the different Bragg reflections,

$$\sigma_{sum} = \sum_{hkl}\left(\frac{1}{\sigma_{f_{hkl}}^{2}} + \frac{1}{\sigma_{p_{hkl}}^{2}}\right), \quad (2)$$

$$f_{hkl}^{the} = \sqrt{Re(Z)^2 + Im(Z)^2}, \quad (3)$$

$$p_{hkl}^{the} = \text{atan}\left(\frac{Im(Z_{hkl})}{Re(Z_{hkl})}\right), \quad (4)$$

$$Z_{hkl} = \exp\left(i2\pi D \cdot H\right), \quad (5)$$

$$D = [a',b',c'], \quad (6)$$

$$H = \begin{bmatrix} h \\ k \\ l \end{bmatrix}, \quad (7)$$

and *a'*, *b'* and *c'* define the position of the absorber atom with respect to the primitive translation vectors, **a**, **b** and **c** of the substrate unit cell. These positions are related to the surface $[1\bar{1}0]$ (x), $[\bar{1}\bar{1}2]$ (y) and $[111]$ (z) directions by:

$$a' = \frac{z}{\sqrt{3}} + \frac{x}{\sqrt{2}} - \frac{y}{\sqrt{6}}, \quad (8)$$

$$b' = \frac{z}{\sqrt{3}} - \frac{x}{\sqrt{2}} - \frac{y}{\sqrt{6}}, \quad (9)$$

$$c' = \frac{z}{\sqrt{3}} + \frac{2y}{\sqrt{6}}. \quad (10)$$

The two iminic N atoms in the molecule are related by a mirror reflection across the $[\bar{1}\bar{1}2]$ direction of the substrate, sharing its the point group symmetry (3mm), and thus could be modelled by a single symmetrically equivalent adsorption site. By contrast, the two aminic N atoms in each molecule are not in symmetrically equivalent sites relative to the point group symmetry of the substrate, so these were modelled by two sites mirrored across the $[1\bar{1}0]$ direction (i.e. by inverting the y coordinate):

$$D = \begin{bmatrix} a' & b' & c' \\ a'' & b'' & c'' \end{bmatrix}, \quad (11)$$

$$a'' = \frac{z}{\sqrt{3}} + \frac{x}{\sqrt{2}} + \frac{y}{\sqrt{6}}, \quad (12)$$

$$b'' = \frac{z}{\sqrt{3}} - \frac{x}{\sqrt{2}} + \frac{y}{\sqrt{6}}, \quad (13)$$

$$c'' = \frac{z}{\sqrt{3}} - \frac{2y}{\sqrt{6}}, \quad (14)$$

and equation 5 becomes:

$$Z_{hkl} = \frac{\sum_{q=0}^{q=n} \exp\left(i2\pi D_q \cdot H\right)}{n}, \quad (15)$$

where *q* is each adsorbate domain on the surface related by the point group symmetry of the substrate and *n* is the number of these symmetrically inequivalent domains. To model this effect of 3mm symmetry of the substrate, and the resulting multiple domains, the calculations were performed on a single 'domain' but including all symmetrically equivalent reflections for the $(\bar{1}11)$ and (200) reflections. Specifically for the $(\bar{1}11)$ reflection, the $(1\bar{1}1)$ and $(11\bar{1})$ reflections were

also considered and for the (200) reflection, the (020) and (002) reflections were also considered. Thus, equation 7 would become:

$$H = \begin{bmatrix} h & l & k \\ k & h & l \\ l & k & h \end{bmatrix}, \tag{16}$$

and equation 15:

$$Z_{hkl} = \frac{\sum_{r=0}^{r=mq=n} \sum_{q=0} \exp\left(i2\pi D_q \cdot H_m\right)}{n \times m}, \tag{17}$$

where *r* is the number of symmetrically identical reflections and *m* the total number of symmetrically identical reflections.

Through this method the degree of agreement between experiment and theory, for any given x,y,z position on the surface, could be calculated. The agreement for absorber atom sites in a plane parallel to the (111) surface, at specific heights above the surface, are shown in Figs. 3a and 3b for the iminic and aminic species, respectively. The heights above the surface of these 2-D slices correspond to the experimental (111) NIXSW coherent positions of 0.90 and 1.03 for the iminic and aminic species, respectively. These slices contain a set of global minima in χ (χ_{min}), with repeating sets at specific heights above the surface that correspond to (111) coherent positions of $(3w + 0.90)$ and $(3v + 1.03)$, where w and v are any integer value. The uncertainty in χ, σ_χ was estimated to be:

$$\sigma_\chi = \frac{1}{\sigma_{sum}}, \tag{18}$$

and thus the uncertainty in the best fitting position was defined as any position that had a $\chi < \chi_{min} + \sigma_\chi$.

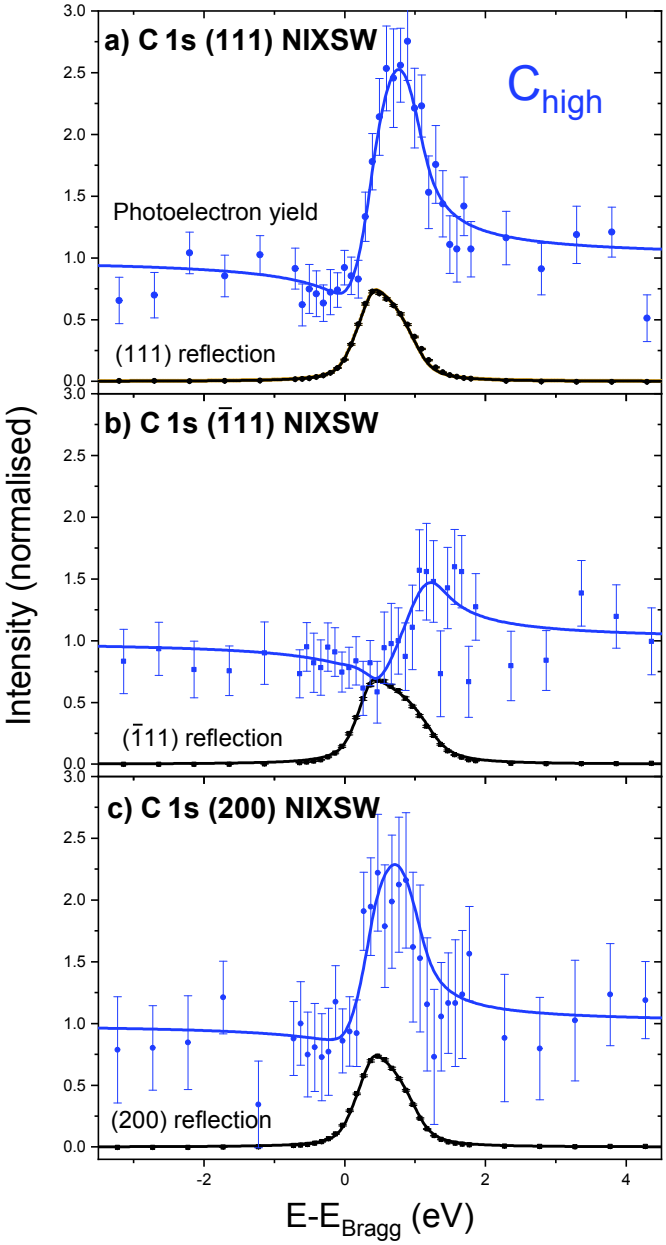

Figure S4. NIXSW measurements for the a) (111), b) $(\bar{1}11)$ and c) (200) reflections for the higher binding energy C 1s peak, C_{high} (see Fig. S1). Values of the coherent positions and coherent fractions for these fits are given in table S1.

Table S1. The fitted coherent fractions, f_{hkl}, and coherent positions, P_{hkl}, for the higher binding energy C_{high} 1s photoemission peak for the (111), $(\bar{1}11)$ and (200) reflections.

	f_{111}	P_{111}	$f_{\bar{1}11}$	$P_{\bar{1}11}$	f_{200}	P_{200}
C_{high}	0.7 ± 0.2	0.07 ± 0.07	0.7 ± 0.2	0.88 ± 0.08	0.4 ± 0.2	0.1 ± 0.1

References:

1. M. Lepper, J. Köbl, T. Schmitt, M. Gurrath, A. de Siervo, M. A. Schneider, H.-P. Steinrück, B. Meyer, H. Marbach and W. Hieringer, *Chemical Communications*, 2017, **53**, 8207-8210.
2. D. Duncan, P. Casado Aguilar, M. Paszkiewicz, K. Diller, F. Bondino, E. Magnano, F. Klappenberger, I. Píš, A. Rubio and J. Barth, *The Journal of Chemical Physics*, 2019, **150**, 094702.

3. D. Woodruff, *Reports on Progress in Physics*, 2005, **68**, 743.
4. C. Fisher, R. Ithin, R. Jones, G. Jackson, D. Woodruff and B. Cowie, *Journal of Physics: Condensed Matter*, 1998, **10**, L623.
5. V. Nefedov, V. Yarzhemsky, I. Nefedova, M. Trzhaskovskaya and I. Band, *Journal of Electron Spectroscopy and Related Phenomena*, 2000, **107**, 123-130.
6. F. Albrecht, F. Bischoff, W. Auwärter, J. V. Barth and J. Repp, *Nano letters*, 2016, **16**, 7703-7709.
7. K. Diller, F. Klappenberger, M. Marschall, K. Hermann, A. Nefedov, C. Wöll and J. Barth, *The Journal of Chemical Physics*, 2012, **136**, 014705.
8. C. Bürker, A. Franco-Cañellas, K. Broch, T.-L. Lee, A. Gerlach and F. Schreiber, *The Journal of Physical Chemistry C*, 2014, **118**, 13659-13666.
9. J. C. Moreno-López, D. J. Mowbray, A. Pérez Paz, R. C. de Campos Ferreira, A. Ceccatto dos Santos, P. Ayala and A. de Siervo, *Chemistry of Materials*, 2019, **31**, 3009-3017.
10. M. Stark, S. Ditze, M. Drost, F. Buchner, H.-P. Steinrück and H. Marbach, *Langmuir*, 2013, **29**, 4104-4110.
11. M. Röckert, M. Franke, Q. Tariq, S. Ditze, M. Stark, P. Uffinger, D. Wechsler, U. Singh, J. Xiao and H. Marbach, *Chemistry–A European Journal*, 2014, **20**, 8948-8953.
12. K. Diller, R. J. Maurer, M. Müller and K. Reuter, *The Journal of Chemical Physics*, 2017, **146**, 214701.